OXFORD

SOT | Society of Toxicology
academic.oup.com/toxsci

TOXICOLOGICAL SCIENCES, 172(2), 2019, 330–343

doi: 10.1093/toxsci/kfz206
Advance Access Publication Date: September 21, 2019
Research Article

Physiologically Based Pharmacokinetic Modeling of Salivary Concentrations for Noninvasive Biomonitoring of 2,4-Dichlorophenoxyacetic Acid (2,4-D)

Alice A. Han,* Charles Timchalk,* Zana A. Carver,* Thomas J. Weber,* Kimberly J. Tyrrell,* Ryan L. Sontag,* Teresa Gibbins,* William B. Chrisler,* Karl K. Weitz,* Dan Du,† Yuehe Lin,† and Jordan N. Smith*,[1]

*Chemical Biology & Exposure Science, Pacific Northwest National Laboratory, Richland, Washington 99354; and †School of Mechanical and Materials Engineering, Washington State University, Pullman, Washington 99164

[1]To whom correspondence should be addressed at Chemical Biology & Exposure Science, Pacific Northwest National Laboratory, PO Box 999, Richland, WA 99354. Fax: (509) 376-9064. Email: Jordan.Smith@pnnl.gov.

ABSTRACT

Saliva has become a favorable sample matrix for biomonitoring due to its noninvasive attributes and overall flexibility in collection. To ensure measured salivary concentrations reflect the exposure, a solid understanding of the salivary transport mechanism and relationships between salivary concentrations and other monitored matrices (ie, blood, urine) is needed. Salivary transport of a commonly applied herbicide, 2,4-dichlorophenoxyacetic acid (2,4-D), was observed *in vitro* and *in vivo* and a physiologically based pharmacokinetic (PBPK) model was developed to translate observations from the cell culture model to those in animal models and further evaluate 2,4-D kinetics in humans. Although apparent differences in experimental *in vitro* and *in vivo* saliva:plasma ratios (0.034 and 0.0079) were observed, simulations with the PBPK model demonstrated dynamic time and dose-dependent saliva:plasma ratios, elucidating key mechanisms affecting salivary transport. The model suggested that 2,4-D exhibited diffusion-limited transport to saliva and was additionally impacted by protein binding saturation and permeability across the salivary gland. Consideration of sampling times post-exposure and potential saturation of transport mechanisms are then critical aspects for interpreting salivary 2,4-D biomonitoring observations. This work utilized PBPK modeling in *in vitro* to *in vivo* translation to explore benefits and limitations of salivary analysis for occupational biomonitoring.

Key words: salivary biomonitoring; 2,4-dichlorophenoxyacetic acid; PBPK modeling.

Biomonitoring provides critical information for assessing environmental and occupational risks by providing a snapshot of chemical exposures in biological samples. Although physiochemical and pharmacokinetic properties of a chemical will dictate which biological matrix is most appropriate for analysis, blood and urine are typically preferred for their accessibility in sample collection. Levels of chemicals measured in these biological matrices can offer valuable insight into the extent of exposure as well as safe concentration ranges that can be further used to develop safety guidelines and regulations (Aylward *et al.*, 2013; Zidek *et al.*, 2017). Coupling biomonitoring information with pharmacokinetic knowledge of a chemical and accounting for physiological features (eg, body weight, blood flow) allows for an informed estimation of the overall external exposure and internal dose (U.S. EPA, 2006).

Although the biomonitoring community considers measured levels of a parent chemical in blood as the gold standard, limitations can impede acquiring and interpreting biomarkers measured in blood. Primarily, it may be difficult to capture the presence of nonpersistent chemicals in blood that are quickly

distributed and metabolized (Needham *et al.*, 2007). In these cases, metabolites can be targeted; however, robust understanding of metabolite pharmacokinetics and specificity of metabolites to the parent compound can be limiting. Urine sampling becomes favorable to monitor chemicals or metabolites that are renally eliminated, but biomarker amounts in spot urine samples can vary based on hydration level, diet, kidney function, age, race/ethnicity, sex (Barr *et al.*, 2005), and chemical elimination kinetics (Aylward *et al.*, 2012). Temporal differences can be an obstacle for both blood and urine biomonitoring, where variation in sampling time points and duration may yield a wide range of measured values (Calafat, 2016). These discrepancies may cause challenges in estimating exposure levels with biomonitoring data and further comparing results within sample populations (Aylward *et al.*, 2012).

Salivary biomonitoring is an emerging alternative with advantages over analyzing other biological matrices. Although peak concentrations measured in saliva are usually lower than blood and urine levels, saliva offers advantages in sampling convenience, capacity for increased sampling frequency, shorter sampling interval, noninvasive nature, cost effectiveness, minimal training required for sample collection, and a greater appeal to subjects. A wide range of targets capable of being detected in saliva include exogenous sources (pesticides, herbicides, drugs, and heavy metals) (Carver *et al.*, 2018; Haeckel and Hanecke, 1996; P'An, 1981; Smith *et al.*, 2017), as well as endogenous biomolecules (hormones, antibodies) (Kaufman and Lamster, 2002). Associations between biomarker or analyte levels found in saliva and other biological matrices are currently ambiguous for many chemicals (Michalke *et al.*, 2015), but elucidating mechanisms driving transport into saliva may help decipher sources of inconsistencies and validate saliva as a viable biomonitoring matrix. Understanding salivary transport mechanisms further provides direction to screen chemicals and predict the capacity and limitations of chemical detection in saliva.

2,4-Dichlorophenoxyacetic acid (2,4-D) is a herbicide of biomonitoring interest due to its prevalent use (30-40 million pounds in the U.S., 2012) (U.S. EPA, 2017) and potential for adverse effects following excessive exposure. Toxicity studies have associated 2,4-D with neurotoxicity (Kim *et al.*, 1994), nephrotoxicity (Tayeb *et al.*, 2012), and carcinogenicity (Garabrant and Philbert, 2002; von Stackelberg, 2013). Pharmacokinetic studies demonstrate rapid elimination of unmetabolized 2,4-D in urine (Kim *et al.*, 1994; Sauerhoff *et al.*, 1977), establishing urine as a practical noninvasive biomonitoring matrix. Relating biomonitoring observations to epidemiological results, however, is a challenge, particularly due to unavailable or unreported information in biomonitoring studies (eg, extent of exposure) (Burns and Swaen, 2012).

Our group recently pioneered an *in vitro* Transwell approach to investigate the transport of small molecules via passive diffusion across a monolayer of cultured salivary gland epithelial cells acquired from Sprague Dawley rats (Carver *et al.*, 2018; Smith *et al.*, 2017; Weber *et al.*, 2017). These studies derived significant transport parameters (eg, protein binding, permeability) from *in vitro* systems to build models predicting the passage of chemicals from plasma to saliva. Recently, Carver *et al.* examined salivary transport of 2,4-D as an alternative to circumvent obstacles associated with urinary or blood biomonitoring and to supplement existing biomonitoring data for better evaluation of the exposure (Carver *et al.*, 2018). Notably, the *in vitro* Transwell cellular system highlighted permeability and protein binding parameters as sensitive contributors driving 2,4-D transport across the salivary gland barrier into the salivary compartment (Carver *et al.*, 2018). Carver *et al.* observed differences between *in vitro* and *in vivo* saliva:plasma ratios, generating uncertainty in *in vitro* to *in vivo* extrapolation of salivary transport (Carver *et al.*, 2018). It was hypothesized that this observation may be attributed to the absence of physiological features (eg, blood flow) under *in vitro* conditions and/or other pharmacokinetic processes not present in conventional cell culture conditions (Carver *et al.*, 2018).

In this study, we developed a physiologically based pharmacokinetic (PBPK) model to examine time- and dose-dependent 2,4-D kinetics in various biological matrices to further explore discrepancies in observed *in vitro* and *in vivo* saliva:plasma ratios. Existing PBPK models were modified to incorporate 2,4-D salivary transport. Accordingly, this work is the first to contribute a salivary component of 2,4-D PBPK modeling that will be able to predict salivary concentrations and offer insight into interpreting biomonitoring observations across sampling matrices.

MATERIALS AND METHODS

Chemicals. 2,4-Dichlorophenoxyacetic acid (2,4-D) (CAS no. 94-75-7), triclopyr (CAS no. 55335-06-3), trimethylsilyldiazomethane (TMSD) (CAS no. 18107-18-1), and other general laboratory chemicals were purchased from Sigma-Aldrich (St Louis, Missouri).

Biological samples. Blood collected from male Sprague Dawley rats was centrifuged at 1600 × g for 10 min to separate plasma and subsequently stored in −70°C. Human plasma (BioReclamation, Westbury, New York, catalog no. HMPLNAHP) was purchased.

2,4-D protein binding. 2,4-D protein binding was measured in rat and human plasma. In these experiments, dilution of plasma in phosphate buffered saline (PBS) was necessary to decrease protein concentration and allow protein binding saturation. 2,4-D was spiked into approximately 2% diluted rat plasma resulting in final concentrations ranging from 7 to 360 μM and into approximately 2% diluted human plasma resulting in final concentrations ranging from 7 to 420 μM. After incubating in 37°C for 1 h, 500 μl aliquots of the spiked plasma were placed in Amicon Ultra Centrifugal Filters (10 kDa cutoff) and centrifuged at 14 000 RFC × g for 20 min. Filtered (unbound concentration fraction) and unfiltered (total concentration) samples were analyzed for 2,4-D (method detailed in "2,4-D quantification" section). Bound 2,4-D concentrations were determined by taking the difference of total and unbound concentrations (total = unbound + bound). Protein binding was described with a 1 (equation 1) or 2 (equation 2) apparent binding site model, where B_{max} is the maximum number of binding sites and k_d is the affinity constant. Models were optimized using a maximum likelihood objective and the Bayesian information criterion (BIC) was used to compare fits. B_{max} values were scaled to total protein concentrations in undiluted plasma. Protein concentrations were determined using the bicinchoninic acid assay with bovine serum albumin as an external standard.

$$C_b = \frac{B_{max} \times C_u}{k_d + C_u} \quad (1)$$

$$C_b = \frac{B_{max1} \times C_u}{k_{d1} + C_u} + \frac{B_{max2} \times C_u}{k_{d2} + C_u}. \quad (2)$$

2,4-D quantification. All samples were analyzed with negative ion chemical ionization by GC-MS, as previously performed (Carver *et al.*, 2018). Triclopyr was used as an internal standard for all 2,4-D quantification in this study. Samples were first acidified with 3 M HCl saturated with NaCl and extracted twice with ethyl acetate. Na_2SO_4 was used to dry sample solutions and the remaining solvent was evaporated under nitrogen stream. Samples were reconstituted in 120 µl of toluene and 80 µl of methanol and derivatized with 20 µl of dimethylsilydiazomethane (TMSD) to produce methyl esters of 2,4-D and triclopyr. Derivatized samples were analyzed with an Rtx-1701 30 m × 0.25 mm id × 0.25 µm df column (Bellefonte, Pennsylvania), Hewlett-Packard (Palo Alto, California) 5973 mass selective detector, and ChemStation data analysis (6890N). Helium was used as the carrier gas at a constant pressure of 24 psi. Initial oven and inlet temperatures were set at 100°C and 210°C, respectively. The oven temperature was ramped 20°C/min to 120°C, then ramped 10°C/min to 260°C, and held for 10 min. 2,4-D and triclopyr derivatives were detected with selective ion monitoring of the quantifiable ions 234 and 273 m/z, respectively. 2,4-D concentrations were quantified with external 2,4-D standard curves prepared in plasma.

Model description. Existing 2,4-D PBPK models simulate 2,4-D kinetics for a wide range of applications. Models are tailored to be suitable for different species (rat, rabbit, human) (Durkin *et al.*, 2004; Kim *et al.*, 1994, 1995), life stage (fetus vs adult) (Kim *et al.*, 1996), or other biological conditions (eg, pregnancy) (Kim *et al.*, 1996) and processes, such as the effect of pH driving protonated and deprotonated species) (Durkin *et al.*, 2004). For the purposes of this work in using PBPK modeling to evaluate noninvasive 2,4-D biomonitoring, a model developed by Kim *et al.* (1994) was modified to incorporate protein binding dependent transport of 2,4-D. The model described by Kim *et al.* addresses the potential neurotoxicity of 2,4-D and accordingly incorporates central nervous system (CNS) compartments such as the brain and cerebral spinal fluid. The model proposed in this paper omitted CNS components, but retained the basic frame of the original model, yielding an 8 compartment model (Figure 1) comprised of arterial and venous blood (protein bound and unbound 2,4-D), body, deep compartment, kidney, blood in salivary gland, salivary glands, and saliva. Differential equations describing the rate of 2,4-D concentration change in each compartment are described in this section. 2,4-D amounts were calculated by taking the integral of the differential equations and concentrations were obtained by dividing 2,4-D amount by compartment volume.

Exposure route. Oral and intravenous (IV) routes of exposure were incorporated in the model with 2,4-D being delivered to the unbound blood compartment. Oral absorption was modeled by a first order rate constant and was optimized for each study as needed. IV exposure was supplied by a bolus dose.

Protein binding. Due to high levels of 2,4-D protein binding (Carver *et al.*, 2018), formation of bound and unbound species in blood was a key component of the model, with only unbound species traversing among compartments. Differential equations describing ligand-protein formation and dissociation were incorporated into the model (equations 3–5). Amount (A) and concentration (C) of unbound 2,4-D (u), bound 2,4-D (b), and unoccupied binding sites (bs) were determined. k_{on} is the second order rate constant of ligand-protein formation, k_{off} is the first order ligand-protein dissociation rate constant, and V_x is

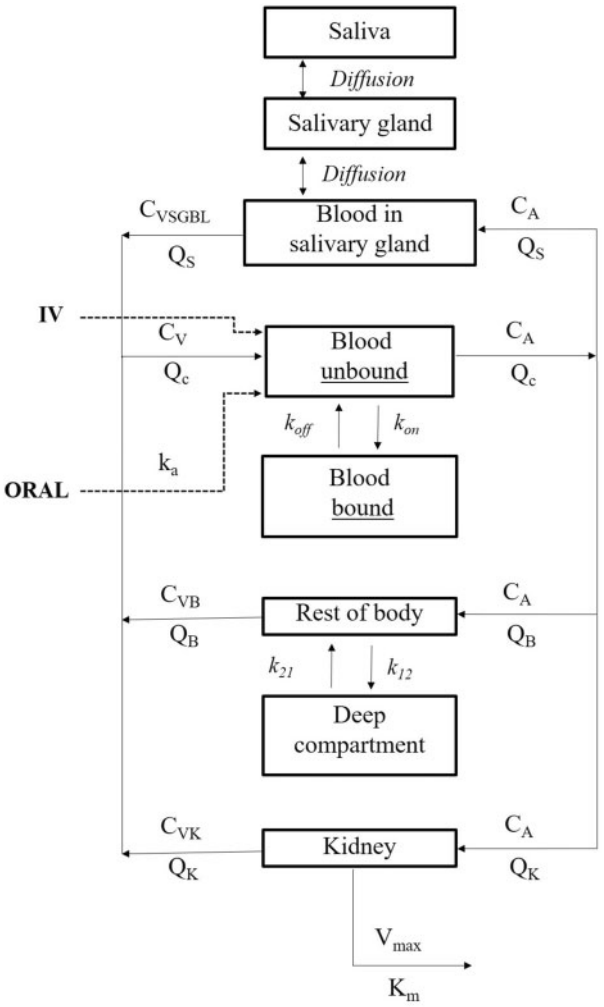

Figure 1. A modified physiologically based pharmacokinetic (PBPK) model of 2,4-dichlorophenoxyacetic acid (2,4-D) consisting of 8 compartments: bound 2,4-D in blood, unbound 2,4-D in blood, blood in salivary gland, salivary gland, saliva, rest of body, deep compartment, and kidney. Salivary transport and protein binding processing were incorporated into a previously published 2,4-D model (Kim *et al.*, 1994).

the volume of the compartment. The affinity constant (k_d) measured in protein binding experiments was used to calculate k_{off}, where the ratio of k_{off}/k_{on} is equal to k_d. The maximum binding capacity (B_{max}), reported as amount per mg protein (nmol/mg) in Table 1, was scaled to plasma protein concentration. The maximum number of binding sites (umol) was determined by normalizing to plasma volume.

$$\frac{dA_u}{dt} = (-k_{on} \times C_u \times C_{bs} + k_{off} \times C_b) \times V_x \quad (3)$$

$$\frac{dA_b}{dt} = (k_{on} \times C_u \times C_{bs} - k_{off} \times C_b) \times V_x \quad (4)$$

$$\frac{dA_{bs}}{dt} = (-k_{on} \times C_u \times C_{bs} + k_{off} \times C_b) \times V_x \quad (5)$$

Blood compartment. Bound and unbound 2,4-D concentrations in blood were defined with protein binding kinetics described in

Table 1. Protein Binding Parameters

Parameter		Rat	Human	Reference
Maximum amount of binding sites (nmol/mg) no. 1	B_{MAX1}	42.6	13.9	Measured; scaled to protein concentration
Maximum amount of binding sites (nmol/mg) no. 2	B_{MAX2}	NA	103.4	Measured; scaled to protein concentration
Binding affinity constant (μM) no. 1	k_{d1}	94.2	18.4	Measured
Binding affinity constant (μM) no. 2	k_{d2}	NA	857.0	Measured
Second order rate constant of protein binding (1/M/s)	k_{on}	1 E06	1 E06	Estimated (Smith *et al.*, 2017)
Protein concentration (plasma) (mg/ml)		50.7	61.3	Measured

the *Protein binding* section. The rate of change in the blood (unbound) compartment is expressed as:

$$\frac{dBL_u}{dt} = Q_C * (C_V - C_A) + \frac{dA_u}{dt}, \quad (6)$$

where Q_C is cardiac output (l/h), C_V is unbound 2,4-D concentration in venous blood, and C_A is unbound 2,4-D concentration in arterial blood (equation 6).

Salivary compartment

The salivary component of the model was divided into 3 subcompartments: blood in salivary gland, salivary gland, and saliva. Previous studies simulated small organic acid transport from plasma to saliva via passive diffusion through the salivary gland (Carver *et al.*, 2018; Smith *et al.*, 2017; Weber *et al.*, 2017) and this mechanism was also adopted for this current model. Differential equations depicting Fick's Law of diffusion were used, where *A* is the amount (μmol), *t* is time (h), PA is the permeability coefficient (cm/h), SA_{SG} is the surface area of salivary gland cells (cm^2), *C* is the concentration (μmol/l), P_{SGBL} is the salivary gland/blood partition coefficient, and P_{SGSL} is the salivary gland: saliva partition coefficient (equations 7–9). 2,4-D concentrations in the salivary gland and saliva were dependent on diffusion. Levels in salivary gland blood were also regulated by cardiac flow to the salivary tissue (Q_{SG}) and unbound 2,4-D concentration in the arterial (C_A) and venous blood (C_{VSGBL}). 2,4-D was cleared from the saliva compartment as a function of the salivary flow rate (Q_{SAL}) and concentration in saliva (C_{SAL}) (equation 10).

$$\frac{dA_{SGBL}}{dt} = Q_{SG} * (C_A - C_{VSGBL}) - PA \times SA_{SG} * \left(C_{VSGBL} - \frac{C_{SG}}{P_{SGB}}\right) \quad (7)$$

$$\frac{dA_{SG}}{dt} = PA \times SA_{SG} * \left(C_{VSGBL} - \frac{C_{SG}}{P_{SG}}\right) + PA \times SA_{SG} * \left(C_{SAL} - \frac{C_{SG}}{P_{SGSL}}\right) \quad (8)$$

$$\frac{dA_{SAL}}{dt} = -PA \times SA_{SG} * \left(C_{SAL} - \frac{C_{SG}}{P_{SGSL}}\right) - \frac{dA_{SE}}{dt} \quad (9)$$

$$\frac{dA_{SE}}{dt} = Q_{SAL} * C_{SAL} \quad (10)$$

The pKa of 2,4-D is 2.73, indicating that 2,4-D will primarily exist in the ionized form in physiological conditions. It was assumed that the population of ionized 2,4-D will remain constant as the pH of the compartments involved in modeling salivary transport (blood, saliva, salivary gland) should not be acidic enough to produce nonionized 2,4-D. The Henderson-Hasselbalch equation confirms that the fraction of ionized 2,4-D does not significantly change across a wide pH range. At pH 5, 7, and 9, the fraction of ionized 2,4-D is 0.9947, 0.9999, and 0.9999, respectively. Instead of treating ionized 2,4-D as incapable of crossing the salivary gland barrier, this model considers ionized species to be able to diffuse, but at significantly slower rates (Smith *et al.*, 2010). A previous *in vitro* study observed 2,4-D diffusion across tightly formed junctions in cultured salivary glands, which prevented the passage of a control chemical (Lucifer Yellow). The absence of active transporters was additionally observed (confirmed with competitive incubation with an active transporter substrate, para-aminohippuric acid), further indicating diffusion as the mode of salivary transport (Carver *et al.*, 2018).

Kidney compartment. A kidney compartment was incorporated in the model to facilitate 2,4-D elimination, where the rate of change is directed by the cardiac flow to the kidney (Q_K), arterial blood concentration (C_A), concentration leaving the kidney in venous blood (C_{VKF}), and rate of elimination (equation 11). The rate of saturable elimination via the kidney (equation 12) is defined by 2,4-D concentration in venous blood leaving the kidney and Michaelis-Menten parameters, V_{max} (maximum elimination rate) and k_m (venous 2,4-D concentration leaving kidney at 50% of maximum elimination rate). Urinary 2,4-D concentration (μmol/l) (equation 13) was estimated by dividing the rate of elimination (μmol/h) (equation 12) by the rate of daily urine production (l/h) (equation 14).

$$\frac{dK}{dt} = Q_K * (C_A - C_{VKF}) - \frac{dE}{dt} \quad (11)$$

$$\frac{dE}{dt} = V_{max} * C_{VKF} / (K_m + C_{VKF}) \quad (12)$$

$$\frac{dCE}{dt} = \frac{dE/dt}{dU_{vol}/dt} \quad (13)$$

$$\frac{dU_{vol}}{dt} = \frac{V_{urine,\ 24h}}{24\ h} \quad (14)$$

Body and deep compartment. Body and deep compartments were necessary to capture the terminal clearance phase, as proposed by previous models (Kim *et al.*, 1994, 1995, 1996). First order rate constants were used to describe transport of 2,4-D between the body and deep compartment (equations 15 and 16). The overall rate of change in the body compartment was dictated by cardiac flow to the body (Q_B), influx of 2,4-D from the arterial blood (C_A), efflux of 2,4-D leaving the body in venous blood (C_{VB}), and the interchange between body and deep compartments via transfer constants (k_{12} , k_{21}).

$$\frac{dB}{dt} = Q_B * (C_A - C_{VB}) - k_{12} * A_B + k_{21} * A_{DC} \quad (15)$$

Table 2. Physiological Parameters

Parameter		Rat	Human	Reference
Blood flow				
Cardiac output (l/h/kg^0.75)	Q_C	14	15.6	Brown *et al.* (1997) and ICRP (2002)
Blood flow to kidney (fraction of cardiac output)	Q_K	0.141	0.19	Brown *et al.* (1997) and ICRP (2002)
Blood flow to salivary tissue (fraction of cardiac output)	Q_S	0.002	0.002	Hiramatsu *et al.* (1994)
Blood flow to rest of body (fraction of cardiac output)	Q_B	$1-\sum(Q_{\text{OTHER FRACTIONS}})$	$1-\sum(Q_{\text{OTHER FRACTIONS}})$	
Volume				
Body weight (kg)	BW	0.3	73	
Blood (fraction of BW)	V_{BL}	0.064	0.0767	Lee and Blaufox (1985) and ICRP (2002)
Salivary gland blood (fraction of BW)	V_{SGBL}	0.0005	0.0005	Smith *et al.* (2017)
Salivary gland tissue (fraction of BW)	V_{SG}	0.0021	0.00116	Wells *et al.* (1959) and ICRP (2002)
Kidney (fraction of BW)	V_K	0.0073	0.00425	Brown *et al.* (1997) and ICRP (2002)
Plasma (fraction of BW)	V_{PL}	0.042	0.042	Lee and Blaufox (1985) and Davy and Seals (1994)
Rest of Body (fraction of BW)	V_B	$1-\sum(V_{\text{OTHER TISSUES}})$	$1-\sum(V_{\text{OTHER TISSUES}})$	
Urine (L) produced in 24 h	V_u	3.3 ml/100 g day	1.7 L (adult male)	Johns Hopkins University ACUC, (2019) and Van Haarst *et al.* (2004)

$$\frac{dDC}{dt} = k_{12} * A_B - k_{21} * A_{DC} \quad (16)$$

Model parameters. Model parameters included physiological and chemical-specific values that were experimentally measured, computationally optimized, extrapolated from previously published data, or derived from PBPK parameter estimation algorithms (Tables 1–4). Physiological features (eg, body compartment volumes, blood flow) of adult rats and humans were acquired from published literature (Brown *et al.*, 1997; Davy and Seals, 1994; Hiramatsu *et al.*, 1994; ICRP, 2002; Johns Hopkins University ACUC, 2019; Lee and Blaufox, 1985; Smith *et al.*, 2017; van Haarst *et al.*, 2004; Wells *et al.*, 1959). Cardiac output was allometrically scaled: $14 \times (BW)^{0.75}$ (rat), $15.6 \times (BW)^{0.75}$ (human).

Pharmacokinetic parameters specific to 2,4-D consisted of partition coefficients, permeability, elimination rates, transfer rates, and protein binding. Partition coefficients were determined with a tissue: blood predicting algorithm for organic chemicals utilizing the Ko/w and tissue lipid contents (Poulin and Krishnan, 1995). A logKo/w of 0.177 (pH 7) (NPIC, 2019) was used to predict partition coefficients. Partitioning occurring between the body and blood was estimated with muscle tissue representing the body compartment. Partition coefficients related to salivary transport were estimated from previously published *in vitro* Transwell experiments (Carver *et al.*, 2018). Briefly, 2,4-D transport from a basolateral "plasma" chamber to an apical "saliva" chamber across a cultured monolayer of salivary gland epithelial cells was allowed to transpire to equilibrium for up to 24 h. Quantified 2,4-D concentrations in cells and in media from basolateral and apical chambers were used to determine salivary partition coefficients. As the formation of unbound 2,4-D species is important for salivary transport, the salivary gland: plasma coefficient was adjusted to reflect unbound 2,4-D partitioning occurring between salivary gland and blood. Flanagan *et al.*, found 2,4-D plasma: whole blood distribution ratios of approximately 2 (Flanagan and Ruprah, 1989), indicating 2,4-D partitioning is primarily distributed into plasma. Assuming all of 2,4-D partitions into plasma instead of red blood cells, the maximum plasma:blood ratio is in fact 1.8 (where RBC: plasma = 45:55). Accordingly, the salivary gland: plasma coefficient was adjusted by 1.8 to describe tissue: blood partitioning. Permeability was optimized in a previous study (Carver *et al.*, 2018) and the same value was used in this model, with no further optimization required. Protein binding parameters (B_{max} and k_d) were acquired from protein binding studies, as described in the *Protein binding* section.

Some parameters from previous modeling efforts were not applicable to this model due to changes in model structure and corresponding mathematical descriptions. Additionally, we were unable to measure some parameters directly (eg, deep compartment transfer rate constants). As such, we optimized those parameters using 2,4-D concentration time course data. Elimination parameters, Michaelis-Menten saturable maximum elimination rate (V_{max}) and Michaelis-Menten constant for saturable elimination (k_m), were optimized using 2,4-D concentrations in plasma and amounts excreted in urine following oral exposure in rats. Initial parameter values were estimated from rat pharmacokinetic data acquired from previous publications (Durkin *et al.*, 2004). Transfer rates between body and deep compartments (k_{12}, k_{21}) were optimized using 2,4-D concentrations in rat plasma following oral exposure (Durkin *et al.*, 2004). Parameters were optimized with a maximum log likelihood objective using the Quasi-Newton algorithm and a heteroscedasticity value of 1.0. Deep compartment transfer rates and V_{max} were allometrically scaled: $V_{max} \times (BW)^{0.75}$, $k_{12} \times (BW)^{-0.25}$, $k_{21} \times (BW)^{-0.25}$.

Parameter sensitivity analysis. Sensitivity analyses were conducted to evaluate parameter importance in predicting 2,4-D concentrations using the human PBPK model following a single oral RfD of 0.005 mg/kg. For each parameter, sensitivity coefficients were calculated for a 1% change, while holding all other parameters constant. Parameter sensitivity was analyzed in simulating 2,4-D kinetics in plasma, urine, and saliva, as well as the saliva:plasma ratio. Human parameter sensitivity was evaluated as performed by Teeguarden *et al.* (2005). Briefly, sensitivity coefficients were characterized as having low, medium, and high sensitivity: low (values between 0.1 and 0.15), medium

Table 3. 2,4-D Pharmacokinetic Parameters (for Both Rat and Human Model)

Parameter		Value	Reference
Body: blood partition coefficient (unitless)	P_B	0.912	Derived with algorithm (Poulin and Krishnan, 1995)
Kidney: blood partition coefficient (unitless)	P_K	1	Derived with algorithm (Poulin and Krishnan, 1995)
Michaelis-Menten saturable maximum elimination rate (μmol/h/kg$^{0.75}$)	V_{MAX}	30.8	Extrapolated from data Durkin *et al.* (2004)
Michaelis-Menten constant for saturable elimination (μM)	k_m	20	Extrapolated from data Durkin *et al.* (2004)
First order rate of absorption (1/h)	k_a	0.8 (rat); 0.3085 (human)	Kim *et al.* (1994) and Sauerhoff *et al.* (1977)
Transfer rate between body and deep compartment (1/h/kg$^{-0.25}$)	k_{12}	0.009	Extrapolated from data Durkin *et al.* (2004)
Transfer rate between deep compartment and body (1/h/kg$^{-0.25}$)	k_{21}	0.001	Extrapolated from data Durkin *et al.* (2004)

Table 4. Salivary Transport Parameters

Parameter		Rat	Human	Reference
Permeation coefficient (cm/h)	P	0.033	0.033	Carver *et al.* (2018)
Salivary gland: blood (unbound) partition coefficient (unitless)	P_{SGB}	6.14	6.14	Estimated from data Carver *et al.* (2018)
Salivary gland: saliva partition coefficient (unitless)	P_{SGSL}	4.51	4.51	Optimized from data Carver *et al.* (2018)
Capillary surface area in salivary tissues (cm^2/g tissue)	SA_{SG}	512	512	Clough and Smaje (1984)
Salivary flow (l/h)	Q_{SAL}	3.58 E-03	0.0336	Funegard *et al.* (1997) and Rudney *et al.* (1995)
Saliva (fraction of BW)	V_{SAL}	6.57 E-06	6.57 E-06	Rudney *et al.* (1995)

(values between 0.15 and 0.5), and high (values 0.5 and higher). Although all parameters were analyzed, only those in the medium and high groups were reported in figures. Authors may be contacted for additional information regarding unreported sensitivity coefficients. Parameters were additionally characterized as having low, medium, and high uncertainty using criteria outlined by Teeguarden *et al.* (2005). Low uncertainty requires extrapolation of the parameter from the correct species, a coefficient of variation <0.5, or verification in previously published PBPK models. Medium uncertainty is defined as using the correct species, a coefficient of variation >0.5, or scaled from parameters of a different species. Parameters derived with any other method are considered to have high uncertainty.

Software. The model was coded in acslXtreme 3.0.2.1 (Aegis Technology, Huntsville, Alabama). Model parameters were also optimized with acslXtreme. For easy dissemination, the model was translated to be compatible with a publically available software for mathematical modeling and simulation, Magnolia, Version 1.2.2 (Magnolia Sciences, LLC, Orlando, Florida). The model code in docx file is available in Supplementary Material. The model in csl file is also available for distribution (please contact authors). R: A language and environment for statistical computing, version 3.4.4 (R Foundation for Statistical Computing, Vienna, Austria) was used for protein binding analysis.

RESULTS

2,4-D Protein Binding in Rat and Human Plasma

Significant protein binding was observed in rat and human plasma. Protein binding saturation in rat plasma occurred over the concentration range of 7–360 μM 2,4-D, where the protein content in PBS diluted rat plasma was approximately 1.01 mg/ml (total—50.7 mg/ml) (Supplementary Figure 1). Unbound 2,4-D fractions under these conditions ranged from 0.64 to 0.91. The 1-binding site model provided a better fit than the 2-binding site model (BIC = 52.4 vs. 56.8). Although protein binding parameters associated with rat plasma were derived *in vitro*, as specified previously, the protein binding model (Equation 1) was superimposed on top of bound and unbound 2,4-D measured in plasma, *in vivo* (Carver *et al.*, 2018 and additional unpublished data provided by authors) (Figure 2A). The protein binding model generated from *in vitro* derived parameters fit well with *in vivo* data, offering confidence in *in vitro* to *in vivo* extrapolation. Final 2,4-D concentrations of 7–420 μM spiked into diluted human plasma (protein concentration—1.22 mg/ml; total—61.3 mg/ml) yielded a higher degree of protein binding compared to rat plasma with unbound fractions ranging from 0.51 to 0.87 (Figure 2B). The 2-binding site model was used to describe protein binding in human plasma per BIC comparison (43.2 [2 site] vs. 45.2 [1 site]). Protein binding parameters are reported in Table 1. Binding affinity appeared to be higher in human plasma, with an affinity constant (k_{d1}) of 18.4 μM (in the high affinity binding site), compared to 94.2 μM in rat plasma.

2,4-D PBPK Model Development and Validation

The 2,4-D PBPK model described in Materials and Methods section was parameterized and optimized with previously published rat pharmacokinetic data (Durkin *et al.*, 2004). Parameters specific to rat species (Tables 1–4) were incorporated in the model. Simulations of 2,4-D concentration in plasma and amount excreted in urine at 3 oral doses (10, 50, and 150 mg/kg) were obtained and overlaid on top of experimental data (Figure 3). The model was validated with another rat pharmacokinetic dataset (Kim *et al.*, 1994) investigating both bolus oral and intravenous exposures (Supplementary Figure 2).

2,4-D Simulation in Rat Model

Approximately 1 h following oral exposure to 5 different doses of 2,4-D (30–150 mg/kg), plasma and saliva samples from rats were analyzed to explore the processes of salivary transport (Carver *et al.*, 2018). PBPK simulations of 2,4-D concentration in plasma and saliva were estimated over 72 h, accounting for conditions of the *in vivo* study (eg, dose, body weight, sample

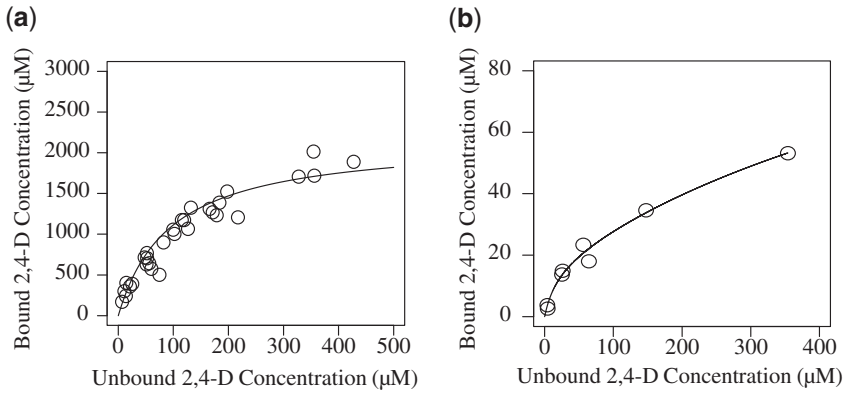

Figure 2. Concentrations of 2,4-dichlorophenoxyacetic acid (2,4-D) bound and unbound to protein in plasma collected from rats following oral exposure (A) and phosphate buffered saline (PBS) diluted human (B) plasma. Lines represent resulting fits to a 1-binding site model (equation 1) in rat plasma (derived from *in vitro* protein binding experiments, as seen in Supplementary Figure 1) and a 2-binding site model (equation 2) in human plasma. Protein binding parameters are reported in Table 1.

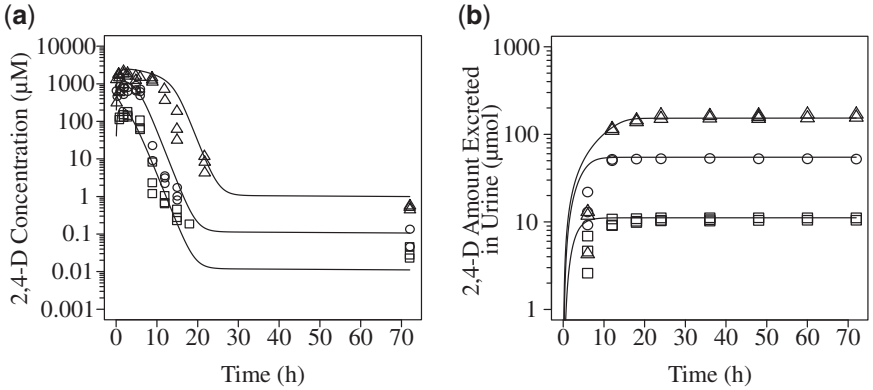

Figure 3. Physiologically based pharmacokinetic (PBPK) model simulations of plasma 2,4-dichlorophenoxyacetic acid (2,4-D) concentration (μM) (A) and amount (μmol) excreted in urine (B) following oral exposure in rats for 72 h and displayed with pharmacokinetic data published in Durkin *et al.* (2004); 10, 50, and 150 mg/kg exposures are represented by square, circle, and triangle markers, respectively.

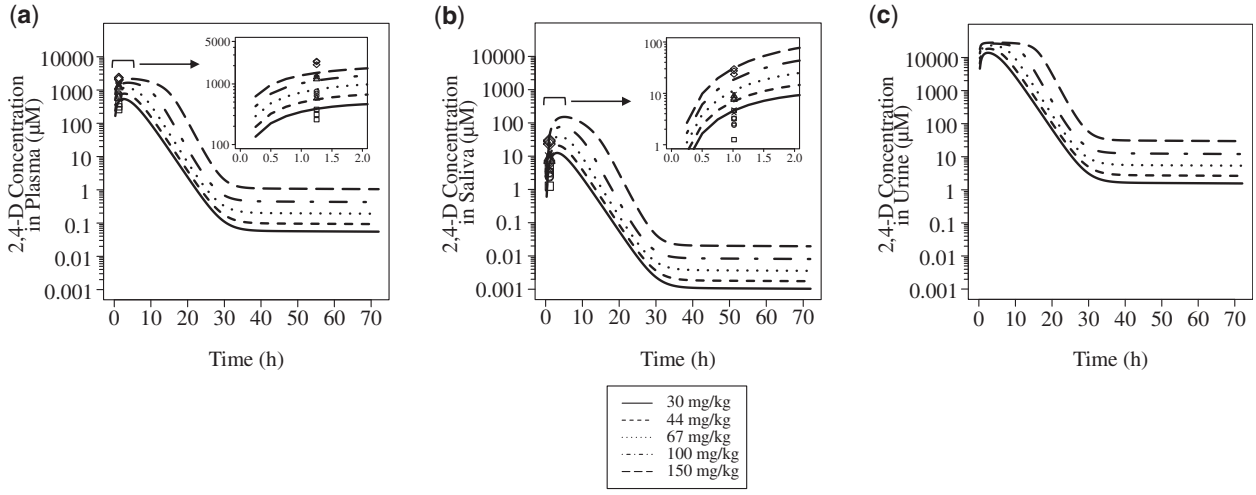

Figure 4. 2,4-Dichlorophenoxyacetic acid (2,4-D) concentration (μM) in plasma (A) and saliva (B) were measured following oral gavage (30–150 mg/kg) in rats 1 h post-administration ($N = 3$ per dose). Data from Carver *et al.* (2018). Resulting 2,4-D concentrations are represented by squares, circles, triangles, x's, and diamonds in order of ascending dose. Lines represent physiologically based pharmacokinetic (PBPK) simulations of 2,4-D concentration in plasma, saliva, and urine (C) from 0 to 72 h. Physiological parameters were adjusted and optimized to mimic specific experimental conditions: increased salivary flow due to pilocarpine ($Q_S = 0.00501$ l/h; measured), decreased cardiac output due to anesthesia ($Q_C = 9.24$ l/h; estimated based on heart rate decrease after anesthesia administration; Olson *et al.*, 1994), oral absorption ($k_a = 0.3085$; optimized).

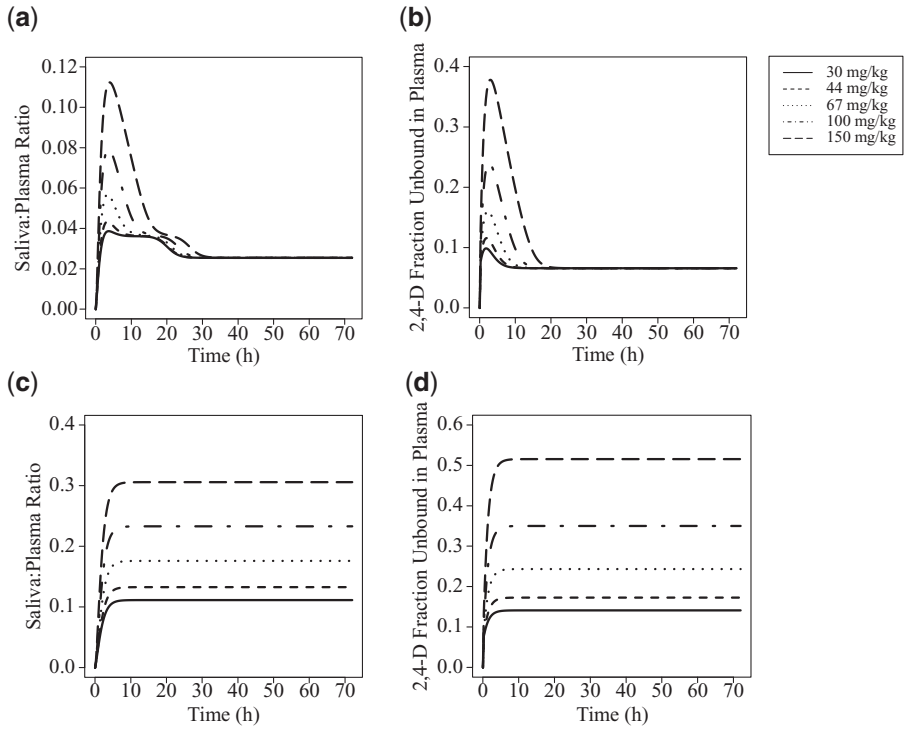

Figure 5. Saliva:plasma ratios (A) and corresponding unbound 2,4-dichlorophenoxyacetic acid (2,4-D) fraction in plasma (B) following oral administration of 2,4-D (30–150 mg/kg) in rats were calculated based on simulated 2,4-D kinetics under normal physiological conditions. Saliva:plasma ratios (C) and corresponding unbound 2,4-D fraction in plasma (D) were also determined in the absence of elimination to evaluate 2,4-D kinetics at equilibrium.

collection time points). Simulations and experimental data demonstrated a dose-response relationship in both saliva and plasma (Figs. 4A and 4B). 2,4-D distribution and clearance in saliva was prominently delayed, compared to 2,4-D kinetics in plasma. Although 2,4-D excretion in urine was not measured, we used the model to predict 2,4-D concentrations in urine (Figure 4C). Estimated urinary concentrations also displayed a dose-dependent response.

The model was used to compare 2,4-D saliva: plasma over time and explore how ratios could be used to interpret biomonitoring observations (Figure 5A). The model predicted dose and time dependent saliva:plasma ratios ranging from 0 to 0.11, peaking around 3–4 h post-exposure. The ratio stabilized at approximately 0.026 for all doses after approximately 30 h postexposure during the terminal elimination phase when protein binding saturation no longer impacts the ratio. Predicted differences in saliva:plasma ratios were driven by protein binding, as fractions of unbound 2,4-D were also dose and time dependent (Figure 5B) and reflected saliva:plasma ratios at the corresponding oral exposures. The contribution of protein binding to saliva:plasma ratios was further demonstrated by the simulation of saliva:plasma ratios and unbound fraction at lower doses, more relevant to human exposures, where protein binding saturation is not a factor (Supplementary Figure 3). Simulations of oral doses at low doses (0.01, 0.1, 1 mg/kg) show dynamic saliva:plasma ratios over time, ranging from 0 to 0.036, but are consistent among these low doses (Supplementary Figure 3A). Unbound 2,4-D fractions (approximately 0.066) were accordingly consistent at the lower doses (Supplementary Figure 3B). With increasing dose, (> 10 mg/kg), a shift in saliva:plasma ratios develops due to corresponding increases in unbound 2,4-D fraction (Supplementary Figure 3B), as a result of 2,4-D protein binding saturation.

To explore other pharmacokinetic impacts on saliva:plasma ratios, clearance processes (renal elimination, salivary clearance, deep compartment transfer) were shut off in the model. 2,4-D concentrations in saliva and plasma rapidly reached equilibrium under these conditions and saliva:plasma ratios and unbound 2,4-D fraction in plasma maintained dose and time dependence (Figs. 5C and 5D), illustrating the significance of protein binding in 2,4-D salivary transport. At equilibrium, saliva:plasma ratios and unbound 2,4-D fraction were slightly higher than the maximum values under normal physiological conditions (Figs. 5A and 5B) due to differences in renal and salivary elimination rates.

A previous publication reported an *in vitro* saliva:plasma ratio of 0.034, whereas the *in vivo* saliva: ratio was observed to be 0.0079 (Carver *et al.*, 2018). To explore this discrepancy, the PBPK model was used to simulate conditions of the *in vitro* experiment. Under physiological *in vitro* conditions the plasma concentration was approximately 190 μM at the time of equilibrium (32 h) (Figure 6B, Carver *et al.*, 2018). An unbound concentration of approximately 3.62 μM in plasma was estimated using the rat protein binding model and parameters reported by Carver *et al.* The PBPK model further predicted a rat oral exposure dose of 1.66 mg/kg that would result in an unbound 2,4-D concentration in plasma of 3.62 μM when clearance processes were shut off to mimic the static conditions of an *in vitro* system (Figure 6B). Following an oral dose of 1.66 mg/kg in a rat model, the saliva:plasma ratio was simulated to be approximately 0.026, comparable to the *in vitro* saliva:plasma ratio of 0.034 ± 0.009 (Figure 6C).

Validation of PBPK Model With Human Exposures

2,4-D levels in plasma and urine resulting from oral exposures in humans were simulated using parameters associated with

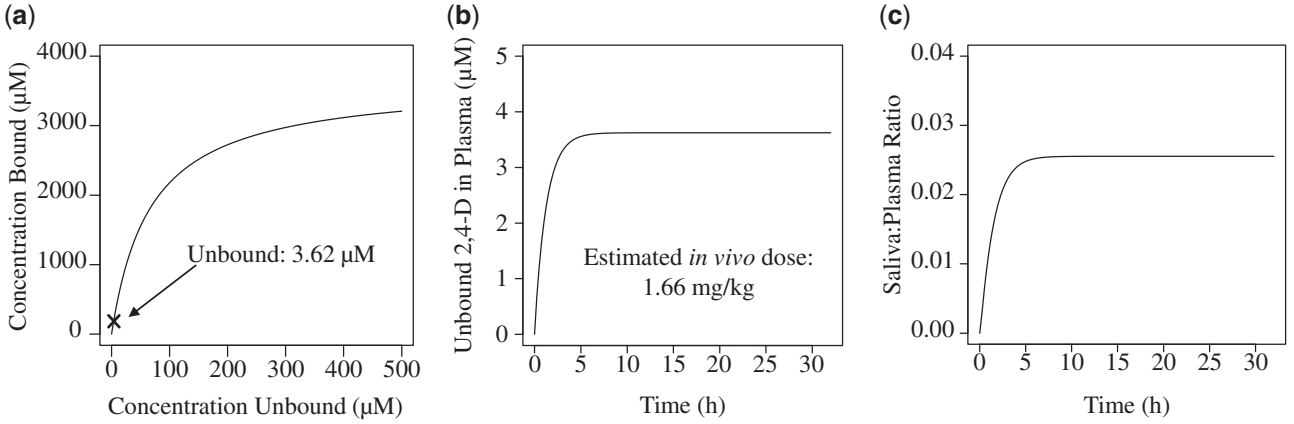

Figure 6. Unbound 2,4-dichlorophenoxyacetic acid (2,4-D) concentration in plasma corresponding to an *in vitro* salivary transport experiment (Carver *et al.*, 2018) was estimated using protein binding parameters and conditions reported by Carver *et al.* ($B_{max} = 51.5$ nmol/mg, $k_d = 67$ μM, protein concentration = 70.6 mg/ml) (A). The PBPK model was used to estimate an *in vivo* rat oral exposure dose of approximately 1.66 mg/kg that resulted in approximately 3.62 μM unbound 2,4-D in the absence of salivary and urinary clearance to mimic *in vitro* conditions (B). Simulations predicted a saliva:plasma ratio of approximately 0.026 in a rat model (C), comparable to an *in vitro* saliva:plasma ratio of approximately 0.034 ± 0.009 (Carver *et al.*, 2018).

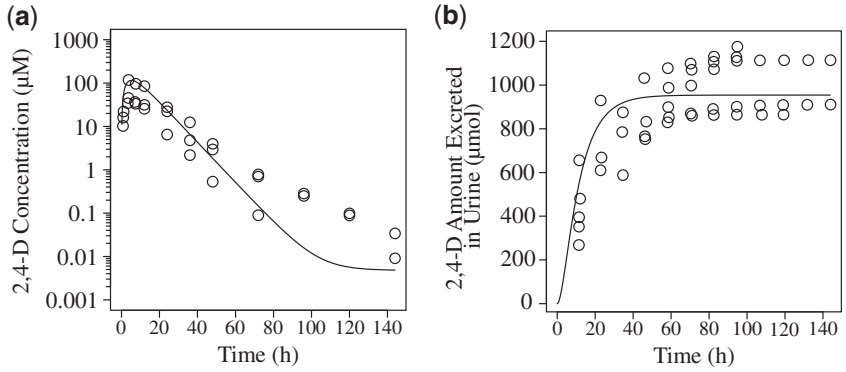

Figure 7. Parameters specific for a human model (Table 1) were applied to the physiologically based pharmacokinetic (PBPK) model and simulations of plasma 2,4-dichlorophenoxyacetic acid (2,4-D) concentration (μM) (A) and amount (μmol) excreted in urine (B) following oral exposure (5 mg/kg) in humans were run from 0 to 144 h. Simulations were validated with pharmacokinetic data collected by Sauerhoff *et al.* (1977) ($N = 3$ plasma; $N = 5$ urine). Subjects were given 1 oral dose of 5 mg/kg. Two subjects ingested 2,4-D in a milk slurry and 3 subjects swallowed 2,4-D with water. Subjects were not fasted prior to the study.

human physiology, as reported in Tables 1–4. To validate the model, predicted values were compared to pharmacokinetic data collected following a 5 mg/kg 2,4-D oral exposure in human subjects ($n = 5$) (Sauerhoff *et al.*, 1977). The model simulates 2,4-D concentrations in plasma and amounts excreted in urine 144 h post-exposure reasonably well (Figure 7).

Simulating 2,4-D Kinetics Following Chronic Exposures in Humans

The PBPK model was used to predict 2,4-D concentrations in saliva, plasma, and urine resulting from chronic exposures in humans. Chronic exposure at the RfD of 0.005 mg/kg/day were simulated for 28 days to allow comparison with currently available biomonitoring equivalents (BE), where BE values were derived from chronic bolus exposure studies in rats (Aylward and Hays, 2008). BE in humans following chronic doses at the RfD are reported as approximately 22.6 nM in plasma and approximately 905 nM in urine Table 10 in Aylward and Hays, 2008. PBPK simulations of 2,4-D concentration in urine were predicted to range between 287 and 1547 nM at steady state, which fit well with the reported urine BE_{RfD} of 905 nM, indicated by the upper dashed line in Figure 8A. PBPK simulations of 2,4-D concentration in plasma were predicted to range between 46 and 248 nM at steady state, significantly higher than the reported BE_{RfD} of 22.6 nM (Figure 8A). 2,4-D concentrations in saliva were estimated to be between 1.16 and 5.28 nM, under the same RfD chronic dosing condition (Figure 8A), indicating that exposures at the RfD would be detectable with current field-deployable sensor technology with a detection limit of 1 ppb (approximately 4.5 nM) (Wang *et al.*, 2017) in saliva approximately 4 h post-exposure.

To gain insight into biomonitoring occupational exposures, the model was used to assess urinary 2,4-D levels measured in samples provided by backpack applicators (Zhang *et al.*, 2011) to estimate exposure doses and further offer predictions and detection capabilities of salivary 2,4-D. The work by Zhang *et al.* reports 2,4-D amounts in 24 h collections of urine following 6 days of applying 2,4-D during a 7–8.5 h workday. The daily quantities of applied 2,4-D were consistent except on days 1 and 6, where workers only applied two-third of what was applied on days 2–5 (Table 2 in Zhang *et al.*, 2011). The PBPK model was used to estimate daily exposure doses of 0.008 mg/kg/day (days 1 and 6) and 0.012 mg/kg/day (days 2–5) based on an average urinary concentration of approximately 2410 nM (assuming daily urine production of 1.7 l) on days 2–5 (Table 6 in Zhang *et al.*, 2011). 2,4-D concentration in urine, plasma, and saliva were simulated by implementing an infusion rate over an approximately 8-h period, followed by approximately 16 h of no exposure (Figure 8B) over 6 days. Predicted 2,4-D concentrations

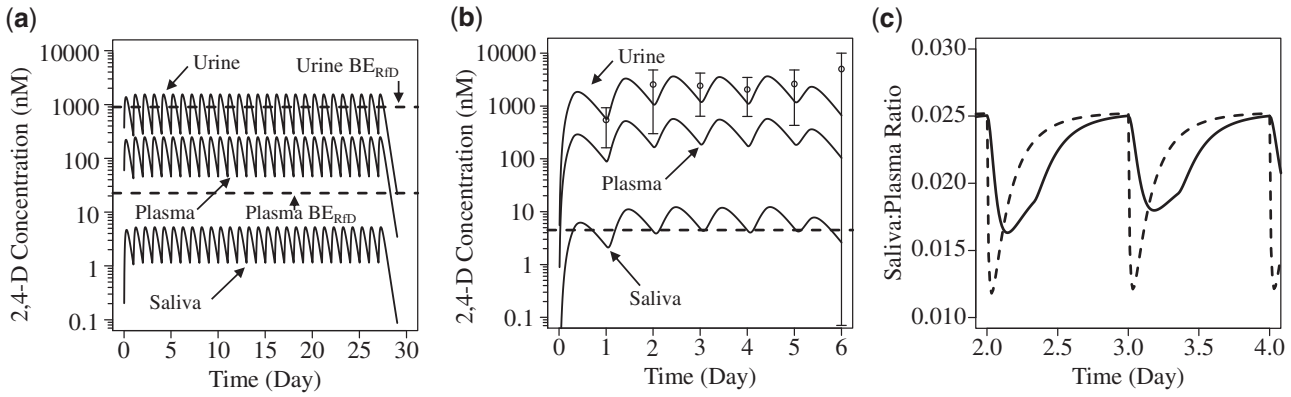

Figure 8. 2,4-Dichlorophenoxyacetic acid (2,4-D) concentrations in saliva, plasma, and urine were simulated in humans following 2,4-D chronic exposure for 28 consecutive days at the RfD (0.005 mg/kg/day). The dashed lines represent urine and plasma biomonitoring equivalents reported by (Aylward and Hays, 2008) (A). Simulations were also run for a 6-day chronic exposure at doses (days 1 and 6: 0.008 mg/kg/day; days 2–5: 0.012 mg/kg/day) predicted from urinary levels (Zhang *et al.*, 2011), where backpack applicators were exposed to 2,4-D over an 8-h workday. The dashed line represents a detection limit of 1 ppb or approximately 4.5 nM of a field-deployable 2,4-D sensor device developed by Wang *et al.* (2017). Data points represent 24 h urinary concentrations ±SD estimated from Zhang *et al.* (2011) (B). Saliva:plasma ratios resulting from both dosing conditions (Figs. 8a and 8b) were determined. The dashed line corresponds to the 28-day RfD exposure and the solid line corresponds to the 6 days—8 h exposure simulation (C).

in urine, plasma, and saliva are substantial enough to be detected with available field-deployable sensor technology with a detection limit of 1 ppb (Wang *et al.*, 2017), indicated by the lower dashed line in Figure 8B.

The saliva:plasma ratio resulting from RfD simulations fluctuated between 0.012 and 0.025 (dashed line), whereas the occupational exposure saliva:plasma ratio ranged from 0.016 to 0.025 (solid line) (Figure 8C). The 2 ratios vary temporally and in range due to differences in exposure, where the RfD exposure was simulated as a bolus dose and occupational simulations employed a constant exposure over an 8-h period. In both cases, the exposure dose was low enough not to saturate protein binding processes, producing an upper saliva:plasma ratio limit of 0.025. In other words, if protein binding was saturated (increasing unbound 2,4-D), more 2,4-D would be available for salivary transport, yielding a higher saliva:plasma ratio, as seen in Figure 5A.

Parameter Sensitivity Analysis

Parameter sensitivity was assessed in simulating plasma, saliva, and urine 2,4-D levels in humans and the resulting plasma:saliva ratio, following a single bolus oral RfD (0.005 mg/kg). Only parameters characterized with high and medium sensitivity are discussed. It is important to note that parameter sensitivity is dependent on factors such as dose, route of exposure, conditions of exposure (bolus vs. infusion) and may be different than parameter sensitivity resulting from a single bolus exposure at a relatively low dose. Simulated 2,4-D concentrations in plasma indicated the parameters shown in Figure 9A were found to be highly sensitive, while all other parameters (not shown) had a low impact. The most sensitive parameters were associated with protein binding and elimination. There is medium uncertainty associated with these parameters in providing accurate estimations of 2,4-D concentration, qualified by criteria described in *Parameter Sensitivity Analysis* section. Partitioning between the body and blood, cardiac output, and the first order rate of oral absorption (k_a) were additionally contributing parameters throughout the simulation. Although cardiac output is a well-established parameter, there is low certainty with body: blood partitioning because the parameter was derived with a tissue: blood predicting algorithm. Additionally, the rate of absorption can vary widely, affected by factors such as food (Li *et al.*, 2018), dissolution of the chemical, diffusion, permeability, and stability in the gastrointestinal (GI) environment (Darwich *et al.*, 2010; Martinez and Amidon, 2002) and needs to be tailored accordingly.

The same parameters sensitive in predicting plasma concentration (k_a, protein binding, elimination, cardiac output, body: blood partitioning) also had high sensitivity for simulating salivary concentration (sensitivity coefficients not shown). Other parameters specifically related to salivary transport were highly sensitive in determining salivary 2,4-D (Figure 9B). As expected with low doses, such as the RfD, where salivary transport is primarily limited by diffusion, partitioning between the salivary gland: blood and salivary gland: saliva were sensitive parameters throughout the simulation. Other parameters related to salivary transport (salivary gland tissue surface area, permeability, blood flow to salivary gland, salivary gland volume, gland blood volume) were mostly important in the early phase of the simulation (up to 10 h), which appears to correspond to peak salivary concentrations. There is high confidence with physiological parameters (salivary gland tissue surface area, blood flow to salivary gland, salivary gland volume, gland blood volume) that are specific to humans and have been used in published PBPK models (Smith *et al.*, 2017). There is low certainty with partition and permeation coefficients, which were experimentally measured with rat tissue culture or computationally optimized and requires further investigation to validate.

Similar to parameter sensitivity for simulating 2,4-D in plasma, prediction of amount excreted in urine was driven by k_a, elimination parameters, protein binding parameters, cardiac output, and partitioning between the body and blood. These parameters were sensitive up to the point where the majority of 2,4-D should be eliminated (approximately 40 h post-exposure) (Figure 9C). Cardiac output and partitioning were characterized with medium sensitivity, while k_a, elimination, and protein binding were considered highly sensitive.

Estimations of saliva:plasma ratios were highly driven by protein binding, cardiac output, salivary gland: blood, and salivary gland: saliva partitioning. Additional physiological parameters related to the salivary gland (salivary gland tissue surface area, salivary gland volume, gland blood volume) and the

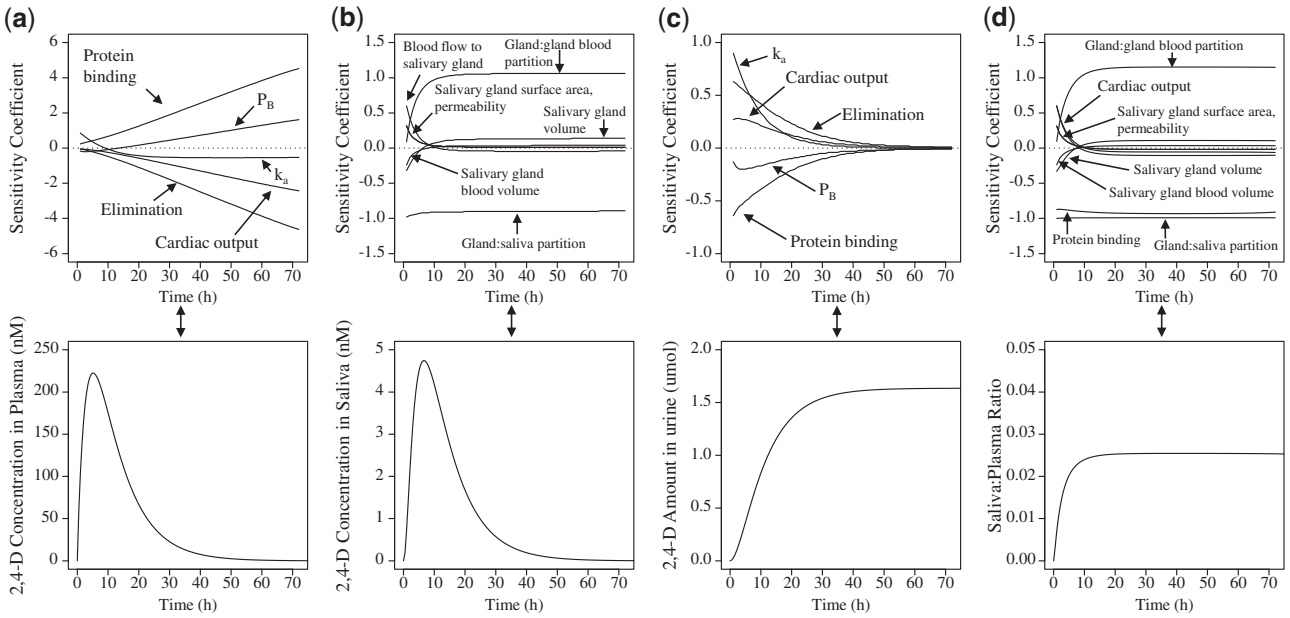

Figure 9. Parameter sensitivity analyses in simulating 2,4-dichlorophenoxyacetic acid (2,4-D) in plasma (A), saliva (B), urine (C), and saliva:plasma ratio (D) in humans following a single RfD (0.005 mg/kg/day) oral dose were conducted. Corresponding 2,4-D levels in plasma, saliva, urine, and saliva:plasma ratio are shown.

computationally optimized permeation coefficient were identified to have medium sensitivity (Figure 9D). All other parameters had low significance in simulating saliva:plasma ratios. As described previously, confidence in these parameters are high for physiological parameters and low for parameters extrapolated from rat data.

DISCUSSION

Exposure assessments, particularly in occupational settings, require regular biomonitoring to prevent excessive contact with hazardous chemicals. Several critical pieces of information are needed to appropriately interpret biomarker levels in the context of the extent of exposure and potential toxicity. Toxicological studies identify hazards, analyze dose-response, and allow regulatory bodies to establish exposure limits [eg, reference doses (RfD) and occupational exposure limits]. Pharmacokinetic knowledge is concurrently needed to estimate detection and temporal limitations of biomonitoring and additionally offers insight into target analytes (parent compound vs metabolite) and suitable biological samples based on the distribution of the chemical within the body. PBPK modeling can assemble these pieces of information together to not only predict internal dosimetry after known administered doses, but further reconstruct external exposures with biomonitoring data (Bartels *et al.*, 2012; Tan *et al.*, 2006).

In the case of 2,4-D exposure, the PBPK model predicted salivary concentrations driven by diffusion-limited transport processes (Figure 4B) and also demonstrated dose and time dependent responses in plasma and urine (Figs. 4A and 4C). 2,4-D is known to have a high affinity for protein (Carver *et al.*, 2018; Rosso *et al.*, 1998) and the model demonstrated the key role of protein binding in dictating the availability and rate of unbound 2,4-D to be transported into saliva (Figure 5B). Consideration of protein binding was especially important for evaluation of high doses (30–150 mg/kg) in animals where protein binding saturation occurred. In human chronic exposure simulations, relevant exposures (0.005–0.012 mg/kg/day) did not encounter protein binding saturation, but should still be examined. Elimination rates were also important in the availability of unbound 2,4-D, demonstrated by the differences in unbound fraction with and without elimination (Figs. 5B and 5D). Then, saturation of elimination rates at higher doses can also impact salivary transport rates. Dynamic transport rates may cause challenges in relating salivary concentrations to other measured biological matrices and further estimate external dose, but understanding the mechanisms that cause dose and time dependent differences in salivary transport can bring more precision to exposure assessments.

The model also predicted variation in 2,4-D saliva:plasma ratios over time in rats (Figure 5A) and humans (Figure 8C) regardless of dose. The relative differences in rates of diffusion-limited transport into saliva and rates of urinary elimination (ie, saliva transport is the rate limiting clearance) drive the temporal variation of the saliva:plasma ratio. In contrast with salivary transport of trichloropyridinol (TCPy), rates of TCPy transport into saliva were faster than rates of urinary elimination (ie, saliva is not the rate limiting clearance), leading to consistent TCPy saliva:blood concentration ratios over the duration of simulations (Smith *et al.*, 2017). Consistent with these results, we observed 2,4-D transport was slower than TCPy transport in the Transwell assay (0.033 vs 0.41 cm/h, respectively) (Carver *et al.*, 2018; Smith *et al.*, 2017). Carver *et al.* measured a higher saliva:plasma ratio *in vitro* using the Transwell assay (0.034 ± 0.009) compared to observed ratio in rats 0.0079 ± 0.0044 (Carver *et al.*, 2018). The discrepancy between the 2 ratios can be explained by a number of processes: (1) The absence of elimination processes in an *in vitro* system, where the *in vitro* saliva:plasma ratio is a representation of a system at equilibrium. (2) Dynamic saliva:plasma ratios over time due to differences in renal clearance rates versus salivary diffusion transport rates. (3) Protein binding differences *in vivo* and *in vitro*. In fact, when the conditions and estimated dose used Carver's *in vitro* system were reproduced with PBPK simulations (Figure 6), the saliva:plasma ratio was estimated to be 0.026, comparable to Carver's 0.034 ± 0.009

ratio. These results further suggest that the dose (and the corresponding unbound 2,4-D fraction) as well as the absence of clearance in an *in vitro* system contributed to the varying saliva:plasma ratios, but can be elucidated with PBPK modeling.

Although consistent saliva:plasma ratios are ideal to back-calculate concentrations in plasma or urine (and ultimately the external dose) from concentrations measured in saliva, identifying and modeling the processes contributing to dynamic ratios can account for differences in experimental or sample collection design. Other studies also corroborate that ratios may vary for a number of reasons, including but not limited to lipophilicity of chemical, protein binding, salivary flow rate, or elimination kinetics (Haeckel, 1993; Michalke *et al.*, 2015). Varying saliva:plasma ratios do not necessarily disqualify a compound for salivary biomonitoring. By understanding that ratios are time- and dose-dependent, they can be used to estimate exposure levels needed to assess potential toxicity and additionally narrow in on an approximate time of exposure. Identifying the underlying processes that can produce different saliva:plasma ratios allow us to apply uncertainty bounds when interpreting biomonitoring observations. For instance, if a certain concentration is detected in saliva, the concentration can be adjusted accordingly by the saliva:plasma ratio range (Figure 8C) to approximate a concentration range in plasma and estimate minimum and maximum exposure doses (assuming 2,4-D exposure is below protein binding saturation concentration). It is also important to note that the temporal profile and range of the ratio can be impacted by dosing conditions (route, duration, frequency), demonstrated by two different exposure condition simulations in Figure 8C. It is then necessary to run an array of simulations reflecting all of the different exposure conditions to capture variability and produce saliva: plasma ranges relevant to a specific exposure.

Different saliva:plasma ratios due to population variation should also be addressed. For instance, if there are significant differences in certain parameters, such the rate of elimination within a population, then the ratio may shift as well. However, parameter sensitivity analysis (Figure 9D) shows that highly sensitive parameters for simulating saliva: plasma should not vary considerably from person to person (ie, the fraction of salivary gland volume per body weight should be consistent within the population). The only sensitive parameter that may vary substantially is cardiac output, which is different for men, women, children, and can also be affected by exercise or digesting food. Simulations were run with cardiac output increased by 3× to mimic increased physical activity or exercise, which produced ratios that are slightly changed, but not considerably: from 0 to 24 h the ratio ranges were 0.0034–0.0025 and 0.0064–0.0025 of simulations run with 1× and 3× cardiac output, respectively (data not shown).

In occupational biomonitoring of humans, a range of maximum salivary concentrations allowed (based on chronic exposure at the RfD) can be modeled to ensure workers are not being exposed to amounts over a safe limit. For additional validation, 2,4-D concentration ranges in plasma and urine can also be predicted (Figure 8A). 2,4-D concentrations in urine simulated by the model agreed well with biomonitoring equivalent (BE) values (following chronic exposure at the RfD), determined by Aylward *et al.*, but modeled concentrations in plasma were higher than the reported plasma BE (dashed lines in Figure 8A) (Aylward and Hays, 2008). Human urine BE_{RfD} was derived with the assumption that the daily intake of 2,4-D at the RfD would be excreted in the 24-h urinary volume. The PBPK model also simulated relatively quick elimination within a 24 h period, leading to agreement between model predictions and BE concentrations. However, human plasma BE_{RfD} was determined by applying uncertainty factors (for intraspecies extrapolation and database uncertainties) to an average rat plasma concentration following administration of a NOAEL POD dose of 5 mg/kg/day for 28 days (Saghir *et al.*, 2006). Through the use of uncertainty factors and extrapolating from animal measurements, the plasma BE_{RfD} may have been underestimated. A PBPK model incorporating human physiology and mechanisms specific to 2,4-D pharmacokinetics may provide a more accurate estimation for biomonitoring assessments.

As the prospect of 2,4-D salivary biomonitoring becomes more feasible and the advantages of its application to bring insight into exposure conditions are identified, being able to measure real time salivary concentrations with field-deployable sensors would be a significant advancement for occupational 2,4-D biomonitoring efforts. Current technology for rapid onsite detection of 2,4-D has been developed and validated with biological samples, capable of capturing levels as low as 1 ppb (approximately 4.5 nM) (Wang *et al.*, 2017). Based on a colorimetric assay coupled to a smartphone readout platform, the sensor is an accessible device where workers only need to supply a small saliva sample and receive minimal instructions to quickly evaluate occupational exposures by comparing measured values to safe ranges designated by the RfD and biomonitoring equivalents. The detection capabilities of the sensor can easily quantify 2,4-D in plasma and urine with RfD (0.005 mg/kg/day) chronic oral exposures and allow salivary monitoring when concentrations are at its peak (Figure 8A), indicating salivary monitoring may be useful for occupational settings, where exposures may exceed the RfD. In fact, biomonitoring data demonstrate a significant level in 24 h urinary collections (Zhang *et al.*, 2011), which our PBPK model predicted an associated exposure dose greater than the RfD (0.008–0.012 mg/kg/day) (Figure 8B). Then, workers that are exposed to 2,4-D daily for a typical 8-h working schedule may be in danger of being exposed to doses exceeding the RfD. Although 2,4-D is rapidly eliminated, caution must be taken when evaluating chronic exposures that are often mixed with other chemicals in an occupational setting, as well as consideration of overall human health and profile (eg, age, pre-existing conditions). Our predictive simulations also indicated that saliva is a promising sample for occupational biomonitoring, as predicted salivary 2,4-D concentrations were above a respectable limit of detection of 1 ppb (Figure 8B).

In conclusion, PBPK modeling was used to predict chemical kinetics, particularly in saliva, and explore many different aspects of biomonitoring, pharmacokinetics, *in vitro* to *in vivo* extrapolation, and animal to human extrapolation. Model simulations demonstrated the advantages and challenges of salivary biomonitoring. Salivary transport processes of the model were parameterized with *in vitro* methods and were successfully extrapolated to model 2,4-D kinetics in rats and humans. The importance of protein binding and 2,4-D permeability across the salivary gland in predicting salivary concentrations was discussed. Exploring saliva:plasma ratios provided insight in using biomonitoring observations to approximate time of exposure and administered dose. Combining field-deployable sensor technology with salivary biomonitoring, PBPK modeling, and knowledge of safe exposure limits can generate rapid information regarding critical exposure conditions needed to maintain appropriate working environments.

SUPPLEMENTARY DATA

Supplementary data are available at *Toxicological Sciences* online.

DECLARATION OF CONFLICTING INTERESTS

The authors declared no potential conflicts of interest with respect to the research, authorship, and/or publication of this article.

FUNDING

This work was supported by CDC/NIOSH grant (R01 OH011023).

REFERENCES

Aylward, L. L., and Hays, S. M. (2008). Biomonitoring equivalents (BE) dossier for 2,4-dichlorophenoxyacetic acid (2,4-D) (CAS No. 94-75-7). *Regul. Toxicol. Pharmacol.* **51**, S37–S48.

Aylward, L. L., Kirman, C. R., Adgate, J. L., McKenzie, L. M., and Hays, S. M. (2012). Interpreting variability in population biomonitoring data: Role of elimination kinetics. *J. Expo. Sci. Environ. Epidemiol.* **22**, 398–408.

Aylward, L. L., Kirman, C. R., Schoeny, R., Portier, C. J., and Hays, S. M. (2013). Evaluation of biomonitoring data from the CDC National Exposure Report in a risk assessment context: Perspectives across chemicals. *Environ. Health Perspect.* **121**, 287–294.

Barr, D. B., Wilder, L. C., Caudill, S. P., Gonzalez, A. J., Needham, L. L., and Pirkle, J. L. (2005). Urinary creatinine concentrations in the U.S. population: Implications for urinary biologic monitoring measurements. *Environ. Health Perspect.* **113**, 192–200.

Bartels, M., Rick, D., Lowe, E., Loizou, G., Price, P., Spendiff, M., Arnold, S., Cocker, J., and Ball, N. (2012). Development of PK- and PBPK-based modeling tools for derivation of biomonitoring guidance values. *Comput. Methods Programs Biomed.* **108**, 773–788.

Brown, R. P., Delp, M. D., Lindstedt, S. L., Rhomberg, L. R., and Beliles, R. P. (1997). Physiological parameter values for physiologically based pharmacokinetic models. *Toxicol. Ind. Health* **13**, 407–484.

Burns, C. J., and Swaen, G. (2012). Review of 2,4-dichlorophenoxyacetic acid (2,4-D) biomonitoring and epidemiology. *Crit. Rev. Toxicol.* **42**, 768–786.

Calafat, A. M. (2016). Contemporary issues in exposure assessment using biomonitoring. *Curr. Epidemiol. Rep.* **3**, 145–153.

Carver, Z. A., Han, A. A., Timchalk, C., Weber, T. J., Tyrrell, K. J., Sontag, R. L., Luders, T., Chrisler, W. B., Weitz, K. K., and Smith, J. N. (2018). Evaluation of non-invasive biomonitoring of 2,4-dichlorophenoxyacetic acid (2,4-D) in saliva. *Toxicology* **410**, 171–181.

Clough, G., and Smaje, L. H. (1984). Exchange area and surface properties of the microvasculature of the rabbit submandibular gland following duct ligation. *J. Physiol.* **354**, 445–456.

Darwich, A. S., Neuhoff, S., Jamei, M., and Rostami-Hodjegan, A. (2010). Interplay of metabolism and transport in determining oral drug absorption and gut wall metabolism: A simulation assessment using the "Advanced Dissolution, Absorption, Metabolism (ADAM)" model. *Curr. Drug Metab.* **11**, 716–729.

Davy, K. P., and Seals, D. R. (1994). Total blood volume in healthy young and older men. *J. Appl. Physiol. (1985)* **76**, 2059–2062.

Durkin, P., Hertzberg, R., and Diamond, G. (2004). Application of PBPK model for 2,4-D to estimates of risk in backpack applicators. *Environ. Toxicol. Pharmacol.* **16**, 73–91.

Flanagan, R. J., and Ruprah, M. (1989). HPLC measurement of chlorophenoxy herbicides, bromoxynil, and ioxynil, in biological specimens to aid diagnosis of acute poisoning. *Clin. Chem.* **35**, 1342–1347.

Funegard, U., Johansson, I., Franzen, L., Ericson, T., Nystrom, H., and Henriksson, R. (1997). Rat salivary gland function after fractionated irradiation. *Acta Oncol.* **36**, 191–198.

Garabrant, D. H., and Philbert, M. A. (2002). Review of 2,4-dichlorophenoxyacetic acid (2,4-D) epidemiology and toxicology. *Crit. Rev. Toxicol.* **32**, 233–257.

Haeckel, R. (1993). Factors influencing the saliva/plasma ratio of drugs. *Ann. N. Y. Acad. Sci.* **694**, 128–142.

Haeckel, R., and Hanecke, P. (1996). Application of saliva for drug monitoring. An in vivo model for transmembrane transport. *Eur. J. Clin. Chem. Clin. Biochem.* **34**, 171–191.

Hiramatsu, Y., Nagler, R. M., Fox, P. C., and Baum, B. J. (1994). Rat salivary gland blood flow and blood-to-tissue partition coefficients following X-irradiation. *Arch. Oral Biol.* **39**, 77–80.

ICRP (2002). Basic anatomical and physiological data for use in radiological protection: Reference values. A report of age- and gender-related differences in the anatomical and physiological characteristics of reference individuals ICRP Publication 89. *Ann. ICRP* **32**, 5–265.

Johns Hopkins University, Animal Care and Use Committee (2019). The Rat. Available at http://web.jhu.edu/animalcare/procedures/rat.html. Accessed September 23, 2019.

Kaufman, E., and Lamster, I. B. (2002). The diagnostic applications of saliva—A review. *Crit. Rev. Oral Biol. Med.* **13**, 197–212.

Kim, C. S., Binienda, Z., and Sandberg, J. A. (1996). Construction of a physiologically based pharmacokinetic model for 2,4-dichlorophenoxyacetic acid dosimetry in the developing rabbit brain. *Toxicol. Appl. Pharmacol.* **136**, 250–259.

Kim, C. S., Gargas, M. L., and Andersen, M. E. (1994). Pharmacokinetic modeling of 2,4-dichlorophenoxyacetic acid (2,4-D) in rat and in rabbit brain following single dose administration. *Toxicol. Lett.* **74**, 189–201.

Kim, C. S., Slikker, W., Jr, Binienda, Z., Gargas, M. L., and Andersen, M. E. (1995). Development of a physiologically based pharmacokinetic model for 2,4-dichlorophenoxyacetic acid dosimetry in discrete areas of the rabbit brain. *Neurotoxicol. Teratol.* **17**, 111–120.

Lee, H. B., and Blaufox, M. D. (1985). Blood volume in the rat. *J. Nucl. Med.* **26**, 72–76.

Li, M., Zhao, P., Pan, Y., and Wagner, C. (2018). Predictive performance of physiologically based pharmacokinetic models for the effect of food on oral drug absorption: Current status. *CPT Pharmacometrics Syst. Pharmacol.* **7**, 82–89.

Martinez, M. N., and Amidon, G. L. (2002). A mechanistic approach to understanding the factors affecting drug absorption: A review of fundamentals. *J. Clin. Pharmacol.* **42**, 620–643.

Michalke, B., Rossbach, B., Goen, T., Schaferhenrich, A., and Scherer, G. (2015). Saliva as a matrix for human biomonitoring in occupational and environmental medicine. *Int. Arch. Occup. Environ. Health* **88**, 1–44.

Needham, L. L., Calafat, A. M., and Barr, D. B. (2007). Uses and issues of biomonitoring. *Int. J. Hyg. Environ. Health* **210**, 229–238.

NPIC (2019). *National Pesticide Information Center: 2,4-D Technical Fact Sheet*. Available at: http://npic.orst.edu/factsheets/archive/2,4-DTech.html#references. Accessed September 23, 2019.

Olson, M. E., Vizzutti, D., Morck, D. W., and Cox, A. K. (1994). The parasympatholytic effects of atropine sulfate and glycopyrrolate in rats and rabbits. *Can. J. Vet. Res.* **58**, 254–258.

P'An, A. Y. (1981). Lead levels in saliva and in blood. *J. Toxicol. Environ. Health* **7**, 273–280.

Poulin, P., and Krishnan, K. (1995). An algorithm for predicting tissue: Blood partition coefficients of organic chemicals from n-octanol: Water partition coefficient data. *J. Toxicol. Environ. Health* **46**, 117–129.

Rosso, S. B., Gonzalez, M., Bagatolli, L. A., Duffard, R. O., and Fidelio, G. D. (1998). Evidence of a strong interaction of 2,4-dichlorophenoxyacetic acid herbicide with human serum albumin. *Life Sci.* **63**, 2343–2351.

Rudney, J. D., Ji, Z., and Larson, C. J. (1995). The prediction of saliva swallowing frequency in humans from estimates of salivary flow rate and the volume of saliva swallowed. *Arch. Oral Biol.* **40**, 507–512.

Saghir, S. A., Mendrala, A. L., Bartels, M. J., Day, S. J., Hansen, S. C., Sushynski, J. M., and Bus, J. S. (2006). Strategies to assess systemic exposure of chemicals in subchronic/chronic diet and drinking water studies. *Toxicol. Appl. Pharmacol.* **211**, 245–260.

Sauerhoff, M. W., Braun, W. H., Blau, G. E., and Gehring, P. J. (1977). The fate of 2,4-dichlorophenoxyacetic acid (2,4-D) following oral administration to man. *Toxicology* **8**, 3–11.

Smith, J. N., Carver, Z. A., Weber, T. J., and Timchalk, C. (2017). Predicting transport of 3,5,6-trichloro-2-pyridinol into saliva using a combination experimental and computational approach. *Toxicol. Sci.* **157**, 438–450.

Smith, J. N., Wang, J., Lin, Y., and Timchalk, C. (2010). Pharmacokinetics of the chlorpyrifos metabolite 3,5,6-trichloro-2-pyridinol (TCPy) in rat saliva. *Toxicol. Sci.* **113**, 315–325.

Tan, Y. M., Liao, K. H., Conolly, R. B., Blount, B. C., Mason, A. M., and Clewell, H. J. (2006). Use of a physiologically based pharmacokinetic model to identify exposures consistent with human biomonitoring data for chloroform. *J. Toxicol. Environ. Health A* **69**, 1727–1756.

Tayeb, W., Nakbi, A., Trabelsi, M., Miled, A., and Hammami, M. (2012). Biochemical and histological evaluation of kidney damage after sub-acute exposure to 2,4-dichlorophenoxyacetic herbicide in rats: Involvement of oxidative stress. *Toxicol. Mech. Methods* **22**, 696–704.

Teeguarden, J. G., Deisinger, P. J., Poet, T. S., English, J. C., Faber, W. D., Barton, H. A., Corley, R. A., and Clewell, H. J. (2005). Derivation of a human equivalent concentration for n-butanol using a physiologically based pharmacokinetic model for n-butyl acetate and metabolites n-butanol and n-butyric acid. *Toxicol. Sci.* **85**, 429–446.

U.S. EPA (2006). Approaches for the application of physiologically based pharmacokinetic (PBPK) models and supporting data in risk assessment (Final Report). U.S. Environmental Protection Agency, Washington, D.C., EPA/600/R-05/043F.

U.S. EPA (2017). Pesticides industry sales and usage: 2008-2012 market estimates. Office of Chemical Safety and Pollution Prevention. EPA.

van Haarst, E. P., Heldeweg, E. A., Newling, D. W., and Schlatmann, T. J. (2004). The 24-h frequency-volume chart in adults reporting no voiding complaints: Defining reference values and analysing variables. *BJU Int.* **93**, 1257–1261.

von Stackelberg, K. (2013). A systematic review of carcinogenic outcomes and potential mechanisms from exposure to 2,4-D and MCPA in the environment. *J. Toxicol.* **2013**, 371610.

Wang, Y., Zeinhom, M. M. A., Yang, M., Sun, R., Wang, S., Smith, J. N., Timchalk, C., Li, L., Lin, Y., and Du, D. (2017). A 3D-printed, portable, optical-sensing platform for smartphones capable of detecting the herbicide 2,4-dichlorophenoxyacetic acid. *Anal. Chem.* **89**, 9339–9346.

Weber, T. J., Smith, J. N., Carver, Z. A., and Timchalk, C. (2017). Non-invasive saliva human biomonitoring: Development of an in vitro platform. *J. Expo. Sci. Environ. Epidemiol.* **27**, 72–77.

Wells, H., Zackin, S. J., Goldhaber, P., and Munson, P. L. (1959). Increase in weight of the submandibular salivary glands of rats following periodic amputation of the erupted portion of the incisor teeth. *Am. J. Physiol.* **196**, 827–830.

Zhang, X., Acevedo, S., Chao, Y., Chen, Z., Dinoff, T., Driver, J., Ross, J., Williams, R., and Krieger, R. (2011). Concurrent 2,4-D and triclopyr biomonitoring of backpack applicators, mixer/loader and field supervisor in forestry. *J. Environ. Sci. Health B* **46**, 281–293.

Zidek, A., Macey, K., MacKinnon, L., Patel, M., Poddalgoda, D., and Zhang, Y. (2017). A review of human biomonitoring data used in regulatory risk assessment under Canada's Chemicals Management Program. *Int. J. Hyg. Environ. Health* **220**, 167–178.